# Pressure induced liquid infiltration in nanopores

A. Han, X. Kong, and Y. Qiao[a)]
*Department of Civil Engineering, University of Akron, Akron, Ohio 44325-3905*

(Received 23 March 2006; accepted 10 May 2006; published online 14 July 2006)

In this article, we report the results of an infiltration/defiltration experiment of a hydrophobic nanoporous silica gel. As the pressure is increased to the critical value, water can be forced into the nanopores. When the pressure is reduced, however, the "outflow" is difficult, leading to a significant hysteresis of sorption isotherm. A first-order thermodynamics analysis is performed to capture the confinement effect of nanopore walls and the mass and energy exchanges between liquid and gas phases in nanopores. © *2006 American Institute of Physics*. [DOI: 10.1063/1.2214368]

## I. INTRODUCTION

The pressure induced infiltration of nanoporous materials has recently received increasing attention. When hydrophobic nanoporous materials are immersed in water at the atmosphere pressure $p_{at}$ due to the capillary effect soaking does not occur spontaneously. As the pressure increases to a critical value $p_{in}$, water can infiltrate into the nanopores, accompanied by a large increase in solid-liquid interfacial energy. When the pressure is reduced back to $p_{at}$, however, the water molecules may not come out of the nanoenvironment, depending on the factors that are still under investigation. According to the limited data currently available in open literature,[1–9] the "nonoutflow" is likely to occur when the pore size is in the mesoporous range (2–50 nm), and the "outflow" is relatively easy if the pore size is smaller than about 1–2 nm.

The conventional interface and microfluidic theories, such as the Washburn type analyses in which the solid-liquid interfaces are assumed to be isolated, have failed in explaining this size effect, as well as the thermal effect,[3] the recovery behavior,[4] the dynamic behavior,[5] the system selectivity,[6] and the gas diffusion phenomenon that will be discussed shortly. In order to model the pressure induced infiltration, a few frameworks, such as the evolution of pore clusters,[7] the flow-direction dependence of contact angle,[8] and the phase transformation with constant system volume and zero gas phase nucleation barrier,[9] have been proposed. However, currently, since the experimental setups are usually sophisticated and the direct observation of infiltration processes is difficult, there are few experimental evidences that can directly support these theories. For instance, at the nanometer scale, the basis of continuum fluid mechanics involved in the effective phase transformation[7] and the flow-direction theory[8] may no longer be valid, and ignoring the system volume change and the energy exchange between gas/liquid phases[9] can be questionable.

## II. EXPERIMENT

In the current study, we designed a simple transparent poly(methylmethacrylate) (PMMA) system so as to directly observe the infiltration/defiltration behaviors of nanoporous particles. The material under investigation was end-capped Fluka 100 $C_8$ reversed phase mesoporous silica with the average pore size $\bar{r}=7.8$ nm and the standard deviation $\delta r=2.4$ nm. The specific pore volume was 560 $mm^3/g$, and the specific surface area was 287 $m^2/g$. The Barrett-Joyner-Halenda (BJH) adsorption characterization measurement was performed at the Quantachrome Instruments. The surface coverage was 10%–12% ($\pm 4$ $\mu mol/m^2$), which led to a high degree of hydrophobicity. The particle size was in the range of 15–35 $\mu$m. Prior to the infiltration tests, the silica particles had been heated in air at 150 °C for 12 h.

The aqueous suspension of 0.5 g of the mesoporous silica particles was sealed in the PMMA cylinder by a stainless steel piston with reinforced gaskets. Initially, no air bubble could be observed. The infiltration experiment was performed using an Instron 5569 machine. The piston was first compressed into the container at a constant rate of 1.0 mm/min. Once the pressure exceeded about 50 MPa, the crosshead was moved back at the same speed. The loading-unloading cycle was repeated until the absorption isotherm curves converged to the steady state, as shown by curves (a) and (b) in Fig. 1, where the specific volume variation is defined as $\Delta V_0/W$, with $\Delta V_0$ being the volume change of the system and $W$ the mass of the silica gel. The system was then thermally treated in a temperature bath in the range of 30–80 °C for 0.5 h either (1) immediately or (2) after resting at room temperature for 6–24 h, followed by another loading-unloading test. The testing results are shown by curves (c) and (d) in Fig. 1, respectively. Altogether four samples were tested.

## III. RESULTS AND DISCUSSION

Curve (a) in Fig. 1 shows that, following the initial linear stage, as the pressure reached the infiltration pressure $p_{in} \approx 17$ MPa, the water was forced into the nanopores, causing the large increase in system compressibility. If the pore size were perfectly uniform, the plateau should be flat. In the current system, due to the pore size distribution, the slope of the absorption isotherm was finite. Eventually, at about 30 MPa, most of the pores were filled and the system compressibility decreased rapidly. The volume variation associated with the plateau region was about 0.55 $cm^3/g$, close to

a)Author to whom correspondence should be addressed; electronic mail: yqiao@uakron.edu

 

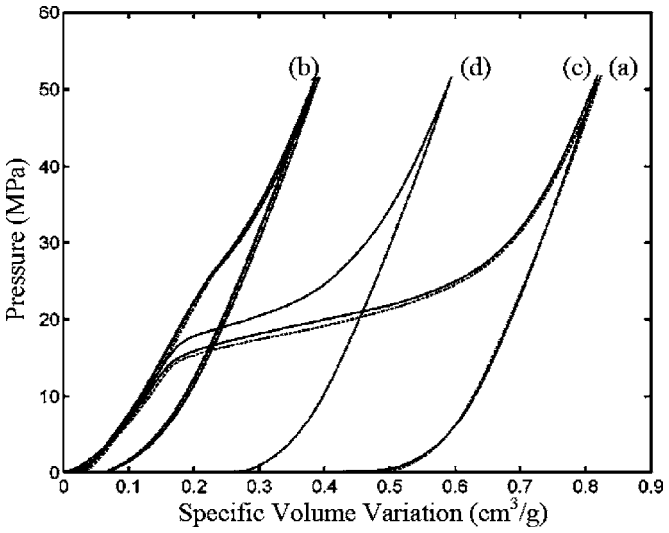


FIG. 1. The sorption isotherm curves: (a) the first loading-unloading cycle (the dashed line); (b) the second (the dotted line), the third, and the fourth loading-unloading cycles without thermal treatment; (c) after the immediate thermal treatment; and (d) after the postponed thermal treatment.

the BJH result of the specific pore volume. As the pressure was reduced, the confined water remained in the nanopores, and thus the unloading curves were quite linear. During the loading-unloading process, there was no significant change in system appearance, except for the variation in volume, indicating that the gas entrapped in the nanopores dissolved in the liquid phase. Since no air bubble could be observed even when the pressure was reduced back to the atmosphere pressure, the gas content in the liquid phase outside the nanoporous particles must be quite constant, that is, the gas molecules remained in the nanopores. Because of the nonoutflow, the extent of infiltration was considerably lowered in the following loading-unloading cycles [see curve (b) in Fig. 1].

When, immediately after the first loading-unloading cycle, the system was thermally treated, the liquid phase was still clear and little air bubbles were formed. However, the energy absorption capacity of the system was recovered significantly [see curve (c) in Fig. 1 and Table I], indicating clearly that after the thermal treatment a certain portion of the porous space was occupied by gas phase. When the temperature exceeded 50 °C, the system could be almost fully recovered.

If, on the other hand, after the first infiltration cycle, the specimen was rested at room temperature under $p_{at}$, the system appearance would change gradually. After 6 h, a large number of air bubbles with the sizes in the range of 0.05–0.5 mm were formed and therefore the sample was no longer transparent. After 24 h, the total volume of the air bubbles was estimated as 0.25 $cm^3/g$, while the energy absorption capacity was still close to zero, suggesting that the nanopores were still filled by liquid. Thermally treating this system would cause a partial recovery, as shown by curve (d) in Fig. 1, where the system recoverability $R_p$ is defined as $E^*_t/E^*_1$, with $E^*_t$ being the absorbed energy in the loading-unloading cycle subsequent to the postponed thermal treatment; the treatment temperature was set to 70 °C; and $t_r$ is the room-temperature resting time. Clearly, during the room-temperature resting, a certain amount of gas molecules diffused out of the nanopores, and the decrease in system recoverability should be attributed to the reduced excess gas content in the nanoenvironment.

TABLE I. The system recoverability $R_s=E^*_2/E^*_1$ as a function of the thermal treatment temperature $T$, where $E^*_i$ is the absorbed energy in the $i$th loading-unloading cycle ($i=1,2$).

| $T$ (°C) | 21 | 30 | 40 | 50 | 70 | 80 |
|---|---|---|---|---|---|---|
| $R_s$ (%) | 11.3 | 24.4 | 45.0 | 94.3 | 97.4 | 97.0 |

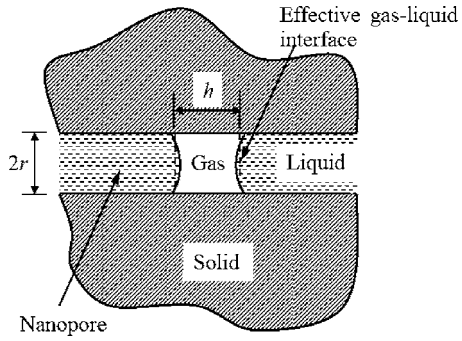


FIG. 2. A schematic diagram of the confined phase transformation in a nanopore.

The motion of the gas-liquid contact line in a nanopore can be considered as the result of expansion or shrinkage of the gas phase.[9] Note that at the nanometer level, sharp liquid-gas interfaces may not exist. Nevertheless, effective boundaries can be defined, e.g., in the context of Gibbs dividing surfaces,[10] as shown in Fig. 2. In an initially filled nanopore, the formation of a gas phase nucleus increases the free energy of system by (a) $\Delta\mu V_G$, where $\Delta\mu$ is the specific nucleation energy and $V_G=\pi r^2 h$ is the volume of the gas phase, with $h$ being the nucleus length; (b) $\gamma_{GL}A_{GL}$, where $\gamma_{GL}$ is the surface tension of the liquid and $A_{GL}=2\pi r^2$ is the gas-liquid interface area; and (c) the external work $p\Delta V$, where $p$ is the applied pressure and $\Delta V=V_G$ is the system volume change. On the other hand, with the nucleation of the gas phase, since the liquid is nonwetting, the liquid-solid interfacial energy is reduced by $\Delta\gamma A_{GS}$, where $\Delta\gamma$ is the difference between the gas-solid and liquid-solid interfacial energies and $A_{GS}=2\pi rh$ is the gas-solid interface area. Note that, if the effective gas-liquid interfaces are irregular, geometry factors should be used in the calculations of $A_{GL}$ and $V_G$, which are ignored in the following discussion for the sake of simplicity.

The thermodynamics equilibrium condition can then be stated as

$$\Delta\mu V_G + \gamma_{GL}A_{GL} + p\Delta V = \Delta\gamma A_{GS}, \tag{1}$$

which can be rewritten as

$$r = r_{cr} \tag{2}$$

or

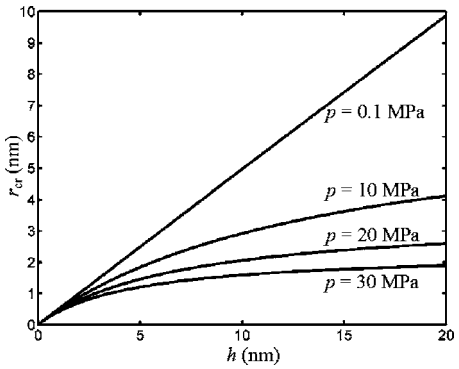


FIG. 3. The relationship between $r_{cr}$ and $h$.

$$h = h_{cr}, \tag{3}$$

where $r_{cr}=2\Delta\gamma/[(p+\Delta\mu)+2\gamma_{GL}/h]$ is the critical pore radius and $h_{cr}=2\gamma_{GL}/[2\Delta\gamma/r-(p+\Delta\mu)]$ is the critical nucleus size of gas phase. According to Eq. (2), when $r<r_{cr}$, the gas phase is stable and can expand spontaneously, which eventually leads to the outflow; when $r>r_{cr}$, the liquid-to-gas phase transformation is energetically unfavorable and therefore the gas phase nucleus will vanish, resulting in the nonoutflow. The relationship between $r_{cr}$ and $h$ is shown in Fig. 3. The value of $\Delta\gamma$ is estimated as $p_{in}\bar{r}/2$, and $\Delta\mu$ is taken as $\mu_0\rho_G$, where $\mu_0=2257.1$ J/kg is the specific energy of evaporation of water and $\rho_G$ is the density of gas phase, which, if we assume that the gas phase follows the law of ideal gas, can be assessed as $\rho_G=\rho_0/(1+p/p_{at})$, with $\rho_0=1.21$ kg/m$^3$ being the air density at $p_{at}$. For the first-order approximation, the macroscopic value of $\gamma_{GL}$, 72 mJ/m$^2$, is used. Figure 3 indicates that decreasing $p$ or increasing $h$ is beneficial to keeping $r<r_{cr}$. According to Eq. (3), there exists an ultimate pore size $r_{ul}=2\Delta\gamma/(p+\Delta\mu)$, at which $h_{cr}\rightarrow\infty$. If $r>r_{ul}$, the outflow is impossible for any $\{\Delta\gamma,\Delta\mu,\gamma_{GL},p\}$.

Based on a Fourier transform infrared (FTIR) spectroscopy analysis, it was confirmed that, at liquid-solid interfaces, there exist a large number of nanometer-scale gas phase nuclei.[11] As temperature rises, the fraction of bigger nuclei increases, i.e., the average $h$ is larger, which explains that, under $p_{at}$, while at room temperature the outflow was negligible, when $T>50$ °C the gas phase nucleation and growth could occur. After the room-temperature resting, however, due to the significant decrease in gas content in the nanopores, the average size of gas phase nuclei was smaller, and therefore the same thermal treatment could cause only a reduced system recovery.

It is clear that the above analysis, which is in the context of mean-field theory, does not constitute a fully developed model. A number of details, such as the kinetics of gas phase nucleation and growth, the possible fragment of gas/liquid phases, and the gas density dependence of $\{\Delta\gamma,\Delta\mu,\gamma_{GL}\}$, are not taken into account. Furthermore, this model can be used only for the outflow process, since the "inflow" is dominated by the kinetics of gas-liquid phase transformation. Nevertheless, it captures the pore size effect on the nonoutflow quite successfully, which provides a scientific basis for further discussion.

## IV. CONCLUDING REMARKS

The pressure induced infiltration of a hydrophobic mesoporous silica gel is investigated. The capillary effect can be overcome as the pressure is increased to a critical value, while the defiltration behavior is much more complicated. The following conclusions are drawn.

(1) In the nanoenvironment, the pore size as well as the mass/energy exchange between gas and liquid phases must be taken into consideration.
(2) The defiltration behavior is affected by pressure, surface and interfacial properties, and thermal treatment history.
(3) There exists a critical pore size above which the "outflow" is energetically unfavorable.

## ACKNOWLEDGMENTS

This work was supported by the Air Force Office of Scientific Research under Grant No. FA9550-06-1-0181, for which the authors are grateful to Dr. Byung-Lip Lee. Special thanks are also due to Dr. Michael Z. Hu for the useful discussions.

[1] V. Eroshenko, R. C. Regis, M. Soulard, and J. Patarin, J. Am. Chem. Soc. **123**, 8129 (2001).
[2] T. Martin, B. Lefevre, D. Brunel, A. Galarneau, F. Di Renzo, F. Fajula, P. F. Gobin, J. F. Quinson, and G. Vigier, Chem. Commun. (Cambridge) **2002**, 24.
[3] X. Kong and Y. Qiao, Philos. Mag. Lett. **85**, 331 (2005).
[4] X. Kong and Y. Qiao, Appl. Phys. Lett. **86**, 151919 (2005).
[5] F. B. Surani, X. Kong, D. B. Panchal, and Y. Qiao, Appl. Phys. Lett. **87**, 163111 (2005).
[6] F. B. Surani, X. Kong, and Y. Qiao, Appl. Phys. Lett. **87**, 251906 (2005).
[7] Y. Qiao and X. Kong, Phys. Scr. **71**, 27 (2005).
[8] V. D. Borman, A. M. Grekhov, and V. I. Troyan, J. Exp. Theor. Phys. **91**, 170 (2000).
[9] B. Lefevre, A. Saugey, J. L. Barrat, L. Bocquet, E. Charlaix, P. F. Gobin, and G. Vigier, J. Chem. Phys. **120**, 4927 (2004).
[10] V. A. Parsegian and R. P. Rand, in *Structure and Dynamics of Membranes*, edited by R. Lipowsky and E. Sackmann (North-Holland, Amsterdam, 1995), p. 643.
[11] J. D. Miller, Y. H. Hu, S. Veeramasuneni, and Y. Lu, Colloids Surf., A **154**, 137 (1999).